Unrestricted Electron Bunching at the Helical Edge

Pavel D. Kurilovich,[1] Vladislav D. Kurilovich,[1] Igor S. Burmistrov,[2] Yuval Gefen,[3] and Moshe Goldstein[4]
[1]Department of Physics, Yale University, New Haven, Connecticut 06520, USA
[2]L. D. Landau Institute for Theoretical Physics, acad. Semenova av. 1-a, 142432 Chernogolovka, Russia
[3]Department of Condensed Matter Physics, The Weizmann Institute of Science, Rehovot 76100, Israel
[4]Raymond and Beverly Sackler School of Physics and Astronomy, Tel Aviv University, Tel Aviv 6997801, Israel

(Received 10 March 2019; published 31 July 2019)

A quantum magnetic impurity of spin S at the edge of a two-dimensional time reversal invariant topological insulator may give rise to backscattering. We study here the shot noise associated with the backscattering current for arbitrary S. Our full analytical solution reveals that for $S > \frac{1}{2}$ the Fano factor may be arbitrarily large, reflecting bunching of large batches of electrons. By contrast, we rigorously prove that for $S = \frac{1}{2}$ the Fano factor is bounded between 1 and 2, generalizing earlier studies.

DOI: 10.1103/PhysRevLett.123.056803

Introduction.—Zero-frequency current noise in a conductor can reveal information about correlations in electronic transport which cannot be extracted from the average current [1,2]. Obtaining information about the correlations requires going beyond linear response (where thermal noise is fully determined by linear conductance through the fluctuation-dissipation theorem), and studying shot noise at voltage larger than the temperature. The ratio between the shot noise and the average current times the electron charge is referred to as the Fano factor. It is useful for characterizing the unit of effective elementary charge in correlated electron systems, e.g., quasiparticle charges in fractional quantum Hall edges [3,4]. Entanglement with an external degree of freedom may modify the effective Fano factor [5,6].

The experimental discovery of 2D topological insulators [7] triggered intensive experimental and theoretical research [8,9]. Electron transport along the helical edge was theoretically predicted to be protected from elastic backscattering by time-reversal symmetry. However, this ideal picture was impugned by transport experiments in HgTe/CdTe [7,10–14] and InAs/GaSb [15–22] quantum wells, Bi bilayers [23], and WTe_2 monolayers [24–26]. In order to explain this data, several physical mechanisms of backscattering were proposed and studied theoretically [27–48].

In contrast to the average current, shot noise at the helical edge has attracted much less experimental and theoretical attention so far [40,49–53]. The shot noise due to backscattering of helical edge electrons via anisotropic exchange (which has to break the conservation of the total z projection of the angular momentum to affect the dc current [29]) with a local spin $S = \frac{1}{2}$ magnetic moment has been calculated in Ref. [52]. The authors of Ref. [52] studied the so-called backscattering Fano factor, F_{bs}, which is the ratio between the zero-frequency noise of the backscattering current, $\mathcal{S}_{\mathrm{bs}}$, and the absolute value of the average backscattering current, $|I_{\mathrm{bs}}|$, in the limit of large voltage bias V. It was found that F_{bs} is bounded between 1 and 2, with the extreme values corresponding to independent backscattering of single electrons and bunched backscattering of pairs of electrons, respectively. The considerations of Ref. [52] were limited to the case of an almost isotropic exchange interaction. This assumption is natural for the model of charge puddles which act as effective spin-$\frac{1}{2}$ magnetic moments [32,35]. However, the spin of a magnetic impurity (MI) can be larger than $\frac{1}{2}$, e.g., $S = \frac{5}{2}$ for a Mn^{2+} ion in a HgTe/CdTe quantum well. Moreover, in the case of a "genuine" MI the exchange interaction is strongly anisotropic [41,46].

In this Letter we study the backscattering shot noise at the edge of a 2D topological insulator mediated by the presence of a single quantum MI. We assume that the impurity is of an arbitrary spin S and the exchange interaction matrix is of a general form. We find the backscattering Fano factor analytically, cf., Eq. (9). Strikingly, for any $S > \frac{1}{2}$ it is not bounded from above, cf., Eqs. (11) and (12); $F_{\mathrm{bs}} > 2$ over a wide parameter range, see Fig. 2. This implies that a dynamical magnetic moment with $S > \frac{1}{2}$ can bunch helical electrons together. Here, in a significant parameter range, for each value of the impurity spin projection S_z electrons are backscattered with a rate $\propto S_z^2$, while S_z itself changes slowly. This results in a modulation of the backscattering events into long correlated pulses [Fig. 1(a)]. For $S = \frac{1}{2}$ this effect is absent [Fig. 1(b)], and we find a concise exact expression for F_{bs} proving rigorously that $1 \leq F_{\mathrm{bs}} \leq 2$, cf., Eq. (10). Our results elucidate an important facet of the dichotomy between topological properties and electronic correlations in one-dimensional edges [54], accounting for mechanisms that break topological protection against backscattering.

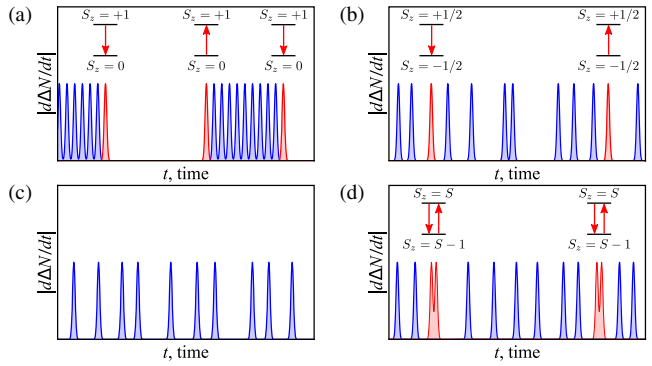

FIG. 1. Sketches of the backscattering current as a function of time in different regimes: (a) $q \ll 1$ and $S = 1$; (b) $q \ll 1$ and $S = 1/2$; (c) $p = 1$; (d) $1 - p \ll 1$. Red and blue peaks correspond to backscattering processes with and without the impurity flips, respectively. Transitions between impurity levels are depicted above each spin-flip process.

Model.—Helical edge electrons coupled to a MI are described by the following Hamiltonian (we use units with $\hbar = k_B = -e = 1$):

$$H = H_e + H_{e-i}, \qquad H_e = iv \int dy \Psi^\dagger(y)\sigma_z \partial_y \Psi(y), \quad (1)$$

where $\Psi^\dagger$ (Ψ) is the creation (annihilation) operator of the edge electrons with velocity v. The Pauli matrices $\sigma_{x,y,z}$ act in the spin basis of the edge states. The exchange electron-impurity interaction is assumed to be local:

$$H_{e-i} = \frac{1}{\nu}\mathcal{J}_{ij} S_i s_j(y_0), \qquad s_j(y) = \frac{1}{2}\Psi^\dagger(y)\sigma_j \Psi(y). \quad (2)$$

Here $\nu = 1/(2\pi v)$ is the density of states per one edge mode, y_0 is the position of the MI, operator S_i denotes the ith component of the impurity spin, and the couplings $\mathcal{J}_{ij}$ are dimensionless and real. We stress that in general the exchange interaction (2) is strongly anisotropic and violates the conservation of the total z projection of the angular momentum of the system [41,46,55]. The latter violation is required to generate persistent backscattering of helical electrons. We assume that the coupling constants are small, $|\mathcal{J}_{ij}| \ll 1$, and we neglect the local anisotropy $H_{\text{anis}} = \mathcal{D}_{kp} S_k S_p$ of the MI spin which is justified at $|\mathcal{D}_{kp}| \ll \max\{\mathcal{J}_{ij}^2 T, |\mathcal{J}_{ij}| V\}$ [47]. In the absence of the local anisotropy we can rotate the spin basis for S_i bringing the exchange matrix $\mathcal{J}_{ij}$ to a lower triangular form. We thus assume hereinafter that $\mathcal{J}_{xy} = \mathcal{J}_{xz} = \mathcal{J}_{yz} = 0$. In addition, we ensure that $\mathcal{J}_{xx}\mathcal{J}_{yy} > 0$ with a proper rotation.

Cumulant generating function.—The average backscattering current and its zero frequency noise can be extracted from the statistics of the number of electrons backscattered off a MI during a large time interval t: $\Delta N(t) = \Sigma_z(t) - \Sigma_z$, where $\Sigma_z(t) = e^{iHt}\Sigma_z e^{-iHt}$ and $\Sigma_z = \int dy s_z(y)$. The cumulant generating function for ΔN can be written as $G(\lambda, t) = \ln \mathrm{Tr}[e^{i\lambda\Sigma_z(t)} e^{-i\lambda\Sigma_z}\rho(0)]$, where $\rho(0)$ stands for the initial density matrix of the full system [56]. It is convenient to write $G(\lambda, t) = \ln \mathrm{Tr}\rho^{(\lambda)}(t)$, where $\rho^{(\lambda)}(t) = e^{-iH^{(\lambda)}t}\rho(0)e^{iH^{(-\lambda)}t}$ is the generalized density matrix of the system at time t and $H^{(\lambda)} = e^{i\lambda\Sigma_z/2} H e^{-i\lambda\Sigma_z/2}$. Tracing out the degrees of freedom of the helical electrons, we obtain $G(\lambda, t) = \ln \mathrm{Tr}_S \rho_S^{(\lambda)}(t)$, where $\rho_S^{(\lambda)}(t)$ denotes the reduced generalized density matrix of the impurity.

Generalized master equation.—In order to find $G(\lambda, t)$ we derive a generalized Gorini-Kossakowski-Sudarshan-Lindblad equation, which governs the time evolution of $\rho_S^{(\lambda)}(t)$ (see Supplemental Material [57]):

$$\frac{d\rho_S^{(\lambda)}}{dt} = -i[H_{e-i}^{\text{mf}}, \rho_S^{(\lambda)}] + \eta_{jk}^{(\lambda)} S_j \rho_S^{(\lambda)} S_k - \frac{\eta_{jk}^{(0)}}{2}\{\rho_S^{(\lambda)}, S_k S_j\}. \quad (3)$$

Here $H_{e-i}^{\text{mf}} = \mathcal{J}_{zz}\langle s_z\rangle S_z/\nu$ is the mean-field part of H_{e-i} with the average non-equilibrium spin density $\langle s_z\rangle = \nu V/2$. Additionally, we have introduced $\eta_{jk}^{(\lambda)} = \pi T(\mathcal{J}\Pi_V^{(\lambda)}\mathcal{J}^T)_{jk}$, where

$$\Pi_V^{(\lambda)} = \begin{pmatrix} f_\lambda^+(V/T) & -if_\lambda^-(V/T) & 0 \\ if_\lambda^-(V/T) & f_\lambda^+(V/T) & 0 \\ 0 & 0 & 1 \end{pmatrix} \quad (4)$$

and $f_\lambda^\pm(x) = (x/2)(e^{-i\lambda}e^x \pm e^{i\lambda})/(e^x - 1)$.

Below we focus on the regime $V \gg T$. The first term on the right-hand side of Eq. (3) is then much larger than the other two terms. Consequently, one may implement the rotating wave approximation to simplify Eq. (3). Within its framework $\rho_S^{(\lambda)}$ is diagonal in the eigenbasis of H_{e-i}^{mf}, i.e., of S_z. Denoting the impurity state with $S_z = m$ as $|m\rangle$ ($m = S, \ldots, -S$) we obtain a classical master equation for the occupation numbers

$$\frac{d}{dt}\langle m|\rho_S^{(\lambda)}|m\rangle = \sum_{m'=-S}^{S} \mathcal{L}_{mm'}^{(\lambda)}\langle m'|\rho_S^{(\lambda)}|m'\rangle. \quad (5)$$

Here $\mathcal{L}^{(\lambda)}$ is a $(2S+1)\times(2S+1)$ tridiagonal matrix. The tridiagonal form indicates that S_z changes by not more than unity in each elementary scattering process. Nonzero elements of $\mathcal{L}^{(\lambda)}$ are given by $\mathcal{L}_{m+1,m}^{(\lambda)} = e^{-i\lambda}\eta_+[S(S+1) - m(m+1)]/4$, $\mathcal{L}_{m,m+1}^{(\lambda)} = (\eta_-/\eta_+)\mathcal{L}_{m+1,m}^{(\lambda)}$, and $\mathcal{L}_{mm}^{(\lambda)} = -e^{i\lambda}\mathcal{L}_{m+1,m}^{(\lambda)} - e^{i\lambda}\mathcal{L}_{m-1,m}^{(\lambda)} + (e^{-i\lambda} - 1)\eta_{zz}^{(0)} m^2$, where $\eta_\pm = \eta_{xx}^{(0)} + \eta_{yy}^{(0)} \pm i(\eta_{xy}^{(0)} - \eta_{yx}^{(0)})$. It is worthwhile to note that by Eq. (5), the characteristic function of $\langle m|\rho_S^{(\lambda)}|m\rangle$ obeys the Heun equation [61].

Results.—At $\lambda = 0$ Eq. (5) describes the time evolution of populations of the impurity energy levels. Through this

equation we establish that the steady state density matrix of the impurity at $V \gg T$ is given by

$$\rho^{(0)}_{S,\mathrm{st}} \sim \left(\frac{1+p}{1-p}\right)^{S_z}, \qquad p = \frac{2\mathcal{J}_{xx}\mathcal{J}_{yy}}{\mathcal{J}^2_{xx}+\mathcal{J}^2_{yy}+\mathcal{J}^2_{yx}}, \quad (6)$$

The dimensionless parameter p determines the polarization of the impurity; i.e., for $p = 1$ only the state $S_z = S$ is occupied, whereas for $p = 0$ all levels are equally populated. Physically, at $p = 1$, $\mathcal{J}_{xx} = \mathcal{J}_{yy}$, $\mathcal{J}_{yx} = 0$, and the impurity spin can be flipped down only by backscattering an edge electron carrying spin-down. We note, though, that at large voltage the current is carried mainly by spin-up electrons. Thus, a steady state of the impurity is established in which $S_z = S$ with essentially unit probability. At $p < 1$ the impurity spin can be flipped down by electrons with spin-up, resulting in depolarization of the impurity. We stress that $\mathcal{J}_{zx}$ and $\mathcal{J}_{zy}$ do not enter into the expression (6) for p because the corresponding terms in the Hamiltonian do not induce impurity spin flips.

To express I_{bs} and $\mathcal{S}_{\mathrm{bs}}$ in a compact form we introduce two parameters:

$$g = \mathcal{J}^2_{xx}+\mathcal{J}^2_{yy}+\mathcal{J}^2_{yx}+\mathcal{J}^2_{zx}+\mathcal{J}^2_{zy}, \quad q = 1-\frac{\mathcal{J}^2_{zx}+\mathcal{J}^2_{zy}}{g}. \quad (7)$$

Then we find that $\eta_{\pm} = \pi g V(1 \pm p)q/2$ and $\eta^{(0)}_{zz} = \pi g V(1-q)/2$. Notice that $0 < p, q \leq 1$ and $g \ll 1$.

The average backscattering current can be found as $I_{\mathrm{bs}} = \langle \Delta N\rangle/t = -(i/t)\partial G(\lambda,t)/\partial\lambda$, where the limits $t \to \infty$ and $\lambda \to 0$ are assumed. Solving Eq. (5) within the first order perturbation theory in λ, we find

$$I_{\mathrm{bs}} = -\frac{\pi g V}{4}\langle R(S_z)\rangle, \quad (8)$$

where $R(S_z) = qS(S+1) - qpS_z + (2-3q)S_z^2$ and $\langle \ldots\rangle = \mathrm{Tr}(\ldots\rho^{(0)}_{S,\mathrm{st}})$. We note that $\langle R(S_z)\rangle > 0$; hence I_{bs} is negative.

The backscattering current noise at zero frequency is given by the second cumulant of ΔN as $\mathcal{S}_{\mathrm{bs}} = \langle\langle(\Delta N)^2\rangle\rangle/t = -t^{-1}\partial^2 G(\lambda,t)/\partial\lambda^2$ at $t \to \infty$ and $\lambda \to 0$. In order to compute $\mathcal{S}_{\mathrm{bs}}$ from Eq. (5) we employ second order perturbation theory in λ [57]. The noise can be written as $\mathcal{S}_{\mathrm{bs}} = F_{\mathrm{bs}}|I_{\mathrm{bs}}|$, where the backscattering Fano factor reads

$$F_{\mathrm{bs}} = 1 + \frac{4}{q(1-p)}\sum_{n=1}^{2S}\frac{\langle P_n[R(S_z) - \langle R(S_z)\rangle]\rangle^2}{n(2S+1-n)\langle R(S_z)\rangle\mu_n}. \quad (9)$$

Here $P_n = \sum_{m=S-n+1}^{S}|m\rangle\langle m|$ is a projector on the subspace of n impurity states with the largest S_z projection and $\mu_n = \langle S+1-n|\rho^{(0)}_{S,\mathrm{st}}|S+1-n\rangle$. Notice that Eq. (9) implies $F_{\mathrm{bs}} \geq 1$. So far, we considered the model of noninteracting edge states. Accounting for electron-electron interaction results only in the common factor for I_{bs} and $\mathcal{S}_{\mathrm{bs}}$ that leaves F_{bs} intact [57].

The most striking feature of Eq. (9) is the divergence at $q \to 0$ for $0 \leq p < 1$ [cf., Eq. (12)]. It indicates that in general the Fano factor is *unrestricted* from above. The only *exception* is the case of $S = 1/2$, for which Eq. (9) gives

$$F_{\mathrm{bs}}(S = 1/2) = (1-qp^4)/(1-qp^2). \quad (10)$$

This expression indicates that F_{bs} is restricted to the range between 1 and 2 for $S = 1/2$. Equation (10) extends the $p, q \to 1$ result of Ref. [52] to arbitrary values of p and q.

The divergence of F_{bs} at $q \to 0$ for impurities with $S > 1/2$ can be explained on physical grounds. For the sake of simplicity we first consider $S = 1$. The inequality $q \ll 1$ implies $|\mathcal{J}_{zx}|, |\mathcal{J}_{zy}| \gg |\mathcal{J}_{xx}|, |\mathcal{J}_{yy}|, |\mathcal{J}_{yx}|$ and, therefore, the backscattering predominantly happens without spin flips of the impurity. By Fermi's golden rule, the rate of such reflection processes is proportional to S_z^2, rendering the backscattering current $d\Delta N/dt$ very sensitive to the spin state of the impurity. The processes associated with $\mathcal{J}_{xx}$, $\mathcal{J}_{yy}$, and $\mathcal{J}_{yx}$ in H_{e-i} are incapable of producing a significant contribution to $d\Delta N/dt$ on their own, but they can transfer the impurity from one spin state to another, switching efficient backscattering on ($S_z = \pm 1$) and off ($S_z = 0$). Consequently, the backscattering current as a function of time looks like a sequence of long pulses, each consisting of a large number (proportional to $1/q$) of backscattered electrons [see Fig. 1(a)]. This peculiar bunching of helical electrons results in $1/q$ divergence of F_{bs}. For $S > 1$ the backscattering current looks differently because the reflection intensity remains finite between the pulses. Still, many-electron correlations are present in $d\Delta N/dt$: impurity rarely jumps between states of different S_z changing the intensity of backscattering $\propto S_z^2$. As $q \to 0$, impurity backscatters increasingly large number of electrons during its stay in a state with a given S_z, which results in the divergent backscattering Fano factor. We note that for $S = 1/2$ for both spin states $S_z^2 = 1/4$. Because of that $d\Delta N/dt$ has no pulses [see Fig. 1(b)] and F_{bs} is not singular at $q \to 0$.

The exact analytical result (9) for F_{bs} can be expressed as a rational function of p and q for any given value of S. However, even for $S = 1$ such an expression is lengthy. We thus focus on the relevant limiting cases below. For an unpolarized impurity $p = 0$ we find

$$F_{\mathrm{bs}}(p=0) = 1 + (2S-1)(2S+3)(2-3q)^2/(45q). \quad (11)$$

In this regime the Fano factor scales as S^2 at large S. This fact has a simple physical interpretation. Since for $p = 0$

each of the $2S+1$ spin states of the impurity is occupied with the same probability, the dynamics of impurity flips between states with different S_z is diffusive. If the MI starts its motion in a state S_z, on average $\sim S^2$ transitions occur before S_z returns to its initial value. Therefore, approximately S^2 subsequent spin flips of the impurity are correlated. These correlations in the dynamics of the impurity spin are mirrored by the correlations in the electron backscattering and result in the S^2 scaling of F_{bs} at small p.

For an almost fully polarized MI, $1-p \ll 1-q$, Eq. (9) yields

$$F_{\mathrm{bs}}(p\to 1)=1+\frac{(1-p)[(2-3q)S+q-1]^2}{q(1-q)S^3}. \quad (12)$$

As follows from Eq. (12) the Fano factor at $p=1$ is equal to unity for $q<1$. This result is expected since for $p=1$ the spin of a MI is locked to the state $S_z=S$. Therefore, the only allowed backscattering processes occur due to the $\mathcal{J}_{zx}$ and $\mathcal{J}_{zy}$ terms in H_{e-i}, which do not require spin flips of the impurity to scatter helical electrons. Consequently, the impurity does not keep memory about backscattered electrons, which results in a Poissonian single-electron reflection process with $F_{\mathrm{bs}}=1$ [see Fig. 1(c)]. For $1-p \ll 1$, rare two-particle reflections are involved in addition to the single-particle backscattering. They are accompanied by short-time excursions of the impurity spin from the state $S_z=S$ to the state $S_z=S-1$ and lead to the enhancement of the Fano factor above unity [cf., Eq. (12)]. In total, for $1-p \ll 1$ the backscattering of electrons represents superposition of the independent single- and two-particle Poisson processes [see Fig. 1(d)]. For large S the deviation of F_{bs} from unity is additionally suppressed by a factor $1/S$ in the considered limit [cf., Eq. (14)].

The behavior of F_{bs} at the point $q=p=1$ is *nonanalytical* owing to $I_{\mathrm{bs}}=0$. The value of the Fano factor depends on the direction in the (q,p) plane at which this point is approached. For a fixed ratio $(1-p)/(1-q)$, Eq. (9) yields

$$F_{\mathrm{bs}}(q,p\to 1)=\frac{2(1-p)+(1-q)S}{1-p+(1-q)S}. \quad (13)$$

The overall behavior of $F_{\mathrm{bs}}(q,p)$ for different values of S is shown in Fig. 2. For $S=1/2$ [Fig. 2(a)] the backscattering Fano factor is bounded by $1\le F_{\mathrm{bs}}\le 2$. For $S>1/2$ [Figs. 2(b)–2(f)] there is a divergence in F_{bs} in the vicinity of $q=0$. The divergence appears to be more pronounced as S increases. However, this trend breaks down for large S. Equation (9) implies that for $S\gg 1/[p(1-q)(2-3q)]$ the Fano factor behaves as

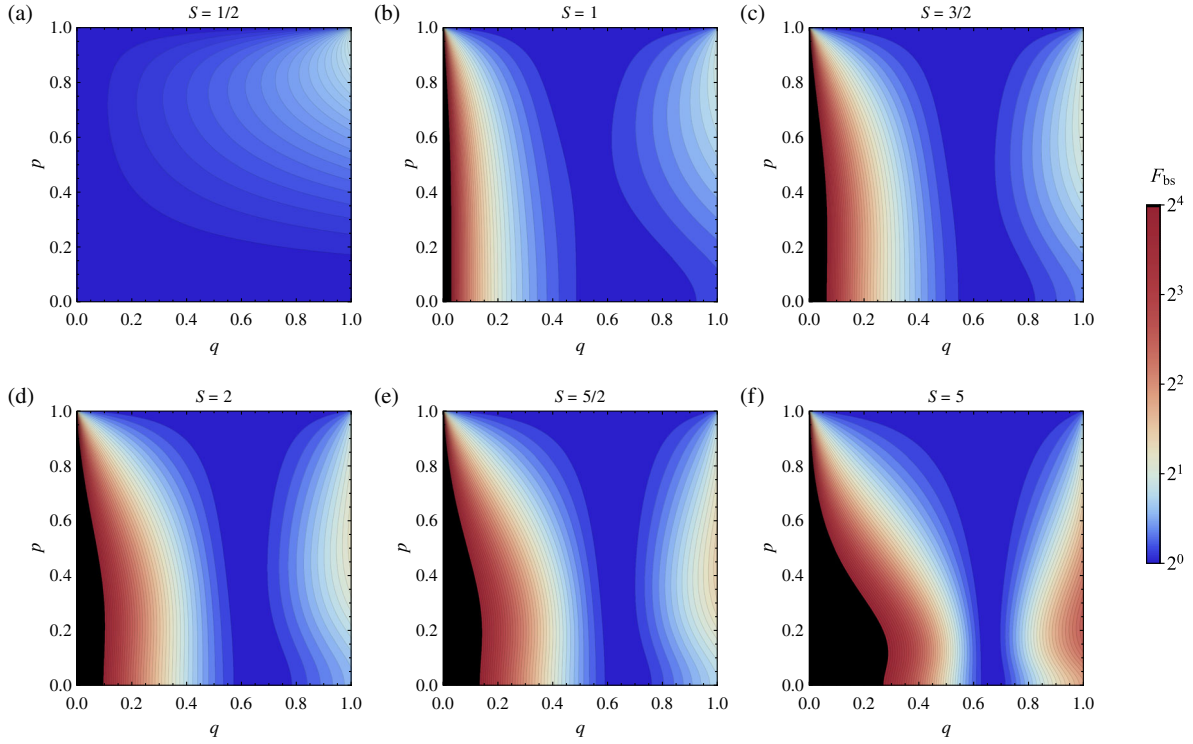

FIG. 2. The backscattering Fano factor as a function of q and p for different values of the spin: (a) $S=1/2$, (b) $S=1$, (c) $S=3/2$, (d) $S=2$, (e) $S=5/2$, (f) $S=5$. Uniform black color corresponds to $F_{\mathrm{bs}}>2^4$. For $S=1/2$, F_{bs} is bounded between 1 and 2. For $S>1/2$, F_{bs} diverges in the limit $q\to 0$, except for the line $p=1$, at which $F_{\mathrm{bs}}=1$.

$$F_{\rm bs} = 1 + \frac{1}{2S}\frac{(1-p^2)(2-3q)^2}{qp^3(1-q)} + O(1/S^2); \quad (14)$$

i.e., it gradually decreases and approaches unity as S gets higher. Thus, the limit of the large spin corresponds to the backscattering of helical electrons by a *classical* MI.

Along with the line $p = 1$ the Fano factor equals unity at the isolated point $(q, p) = (2/3, 0)$. This is universal for all S [see Eq. (11)]. At this point the backscattering rate is independent of the impurity state and, therefore, the backscattering current statistics has a Poissonian single-particle character. The interplay between an S^2 scaling of $F_{\rm bs}$ at $p \to 0$ and the presence of a degenerate point $(q, p) = (2/3, 0)$ results in a bottleneck feature in the vicinity of the latter in Figs. 2(b)–2(f). The $1/S$ term in Eq. (14) cancels at the line $q = 2/3$ and $F_{\rm bs}(q = 2/3) - 1 \sim 1/S^3$ for $p \neq 0$.

Conclusions.—To summarize, we have investigated the zero-frequency statistics of the backscattering current induced by a magnetic impurity of an arbitrary spin S located near the edge of a two-dimensional topological insulator. We addressed the limit of large voltage $|V| \gg \max\{T, |\mathcal{D}_{kp}/\mathcal{J}_{ij}|\}$, where it is possible to neglect the thermal contribution to the noise, as well as the effect of the local anisotropy of the magnetic impurity. Our analytical solution for the average backscattering current and its zero-frequency noise underscores several striking features. (i) The dependence of the average backscattering current and noise on the elements of the exchange matrix is determined by three parameters (g, p, q) only instead of *a priori* six different parameters (the number of nonzero elements of the exchange matrix $\mathcal{J}_{ij}$). (ii) For $S > 1/2$ the backscattering Fano factor can be arbitrary large, diverging in the limit $q \to 0$. This implies that the backscattered electrons can be bunched together in long pulses. Observation of electron bunching is a novel challenge for experimentalists which might shed light on the nature of backscattering at the helical edge, and on how emerging strong correlations can undermine topological protection against backscattering. (iii) For $S = 1/2$ the backscattering Fano factor is limited to the range between 1 and 2. (iv) The backscattering Fano factor is independent of the electron-electron interaction.

We thank V. Kachorovskii for discussions. Hospitality by Tel Aviv University, the Weizmann Institute of Science, the Landau Institute for Theoretical Physics, and the Karlsruhe Institute of Technology is gratefully acknowledged. The work was partially supported by the programs of the Russian Ministry of Science and Higher Education, DFG Research Grant No. SH 81/3-1, the Italia-Israel QUANTRA, the Israel Ministry of Science and Technology (Contract No. 3-12419), the Israel Science Foundation (Grant No. 227/15), the German Israeli Foundation (Grant No. I-1259-303.10), and the US-Israel Binational Science Foundation (Grant No. 2016224), and a travel grant by the BASIS Foundation (Russia).

[1] Ya. M. Blanter and M. Buttiker, Shot noise in mesoscopic conductors, Phys. Rep. **336**, 1 (2000).
[2] G. B. Lesovik and I. A. Sadovskyy, Scattering matrix approach to the description of quantum electron transport, UFN **181**, 1041 (2011) [Phys. Usp. **54**, 1007 (2011)].
[3] L. Saminadayar, D. C. Glattli, Y. Jin, and B. Etienne, Observation of the $e/3$ Fractionally Charged Laughlin Quasiparticle, Phys. Rev. Lett. **79**, 2526 (1997).
[4] R. de-Picciotto, M. Reznikov, M. Heiblum, V. Umansky, G. Bunin, and D. Mahalu, Direct observation of a fractional charge, Nature (London) **389**, 162 (1997); M. Reznikov, R. de-Picciotto, T. G. Griffiths, M. Heiblum, and V. Umansky, Observation of quasiparticles with one-fifth of an electron's charge, Nature (London) **399**, 238 (1999).
[5] C. Birchall and H. Schomerus, Counting Statistics for Mesoscopic Conductors with Internal Degrees of Freedom, Phys. Rev. Lett. **105**, 026801 (2010).
[6] S. Barbarino, R. Fazio, V. Vedral, and Y. Gefen, Engineering statistical transmutation of identical quantum particles, Phys. Rev. B **99**, 045430 (2019).
[7] M. König, S. Wiedmann, C. Brüne, A. Roth, H. Buhmann, L. W. Molenkamp, X.-L. Qi, and S.-C. Zhang, Quantum spin Hall insulator state in HgTe quantum wells, Science **318**, 766 (2007).
[8] X.-L. Qi and S.-C. Zhang, Topological insulators and superconductors, Rev. Mod. Phys. **83**, 1057 (2011).
[9] M. Z. Hasan and C. L. Kane, Colloquium: Topological insulators, Rev. Mod. Phys. **82**, 3045 (2010).
[10] K. C. Nowack, E. M. Spanton, M. Baenninger, M. König, J. R. Kirtley, B. Kalisky, C. Ames, P. Leubner, C. Brüne, H. Buhmann, L. W. Molenkamp, D. Goldhaber-Gordon, and K. A. Moler, Imaging currents in HgTe quantum wells in the quantum spin Hall regime, Nat. Mater. **12**, 787 (2013).
[11] G. Grabecki, J. Wróbel, M. Czapkiewicz, Ł. Cywiński, S. Gierał towska, E. Guziewicz, M. Zholudev, V. Gavrilenko, N. N. Mikhailov, S. A. Dvoretski, F. Teppe, W. Knap, and T. Dietl, Nonlocal resistance and its fluctuations in microstructures of band-inverted HgTe/(Hg, Cd)Te quantum wells, Phys. Rev. B **88**, 165309 (2013).
[12] G. M. Gusev, E. B. Olshanetsky, Z. D. Kvon, O. E. Raichev, N. N. Mikhailov, and S. A. Dvoretsky, Transition from insulating to metallic phase induced by in-plane magnetic field in HgTe quantum wells, Phys. Rev. B **88**, 195305 (2013).
[13] G. M. Gusev, Z. D. Kvon, E. B. Olshanetsky, A. D. Levin, Y. Krupko, J. C. Portal, N. N. Mikhailov, and S. A. Dvoretsky, Temperature dependence of the resistance of a two-dimensional topological insulator in a HgTe quantum well, Phys. Rev. B **89**, 125305 (2014).
[14] E. B. Olshanetsky, Z. D. Kvon, G. M. Gusev, A. D. Levin, O. E. Raichev, N. N. Mikhailov, and S. A. Dvoretsky, Persistence of a Two-Dimensional Topological Insulator State in Wide HgTe Quantum Wells, Phys. Rev. Lett. **114**, 126802 (2015).

[15] I. Knez, R.-R. Du, and G. Sullivan, Evidence for Helical Edge Modes in Inverted InAs/GaSb Quantum Wells, Phys. Rev. Lett. **107**, 136603 (2011).
[16] K. Suzuki, Y. Harada, K. Onomitsu, and K. Muraki, Edge channel transport in the InAs/GaSb topological insulating phase, Phys. Rev. B **87**, 235311 (2013).
[17] E. M. Spanton, K. C. Nowack, L. Du, G. Sullivan, R.-R. Du, and K. A. Moler, Images of Edge Current in InAs/GaSb Quantum Wells, Phys. Rev. Lett. **113**, 026804 (2014).
[18] L. Du, I. Knez, G. Sullivan, and R.-R. Du, Robust Helical Edge Transport in Gated InAs/GaSb Bilayers, Phys. Rev. Lett. **114**, 096802 (2015).
[19] K. Suzuki, Y. Harada, K. Onomitsu, and K. Muraki, Gate-controlled semimetal-topological insulator transition in an InAs/GaSb heterostructure, Phys. Rev. B **91**, 245309 (2015).
[20] S. Mueller, A. N. Pal, M. Karalic, T. Tschirky, C. Charpentier, W. Wegscheider, K. Ensslin, and T. Ihn, Nonlocal transport via edge states in InAs/GaSb coupled quantum wells, Phys. Rev. B **92**, 081303(R) (2015).
[21] T. Li, P. Wang, G. Sullivan, X. Lin, and R.-R. Du, Low-temperature conductivity of weakly interacting quantum spin Hall edges in strained-layer InAs/GaInSb, Phys. Rev. B **96**, 241406(R) (2017).
[22] S. Mueller, C. Mittag, T. Tschirky, C. Charpentier, W. Wegscheider, K. Ensslin, and T. Ihn, Edge transport in InAs and InAs/GaSb quantum wells, Phys. Rev. B **96**, 075406 (2017).
[23] C. Sabater, D. Gosálbez-Martánez, J. Fernádez-Rossier, J. G. Rodrigo, C. Untiedt, and J. J. Palacios, Topologically Protected Quantum Transport in Locally Exfoliated Bismuth at Room Temperature, Phys. Rev. Lett. **110**, 176802 (2013).
[24] Z. Fei, T. Palomaki, S. Wu, W. Zhao, X. Cai, B. Sun, P. Nguyen, J. Finney, X. Xu, and D. H. Cobden, Edge conduction in monolayer WTe_2, Nat. Phys. **13**, 677 (2017).
[25] Z.-Y. Jia, Y.-H. Song, X.-B. Li, K. Ran, P. Lu, H.-J. Zheng, X.-Y. Zhu, Z.-Q. Shi, J. Sun, J. Wen, D. Xing, and S.-C. Li, Direct visualization of a two-dimensional topological insulator in the single-layer $1T' - WTe_2$, Phys. Rev. B **96**, 041108(R) (2017).
[26] S. Wu, V. Fatemi, Q. D. Gibson, K. Watanabe, T. Taniguchi, R. J. Cava, and P. Jarillo-Herrero, Observation of the quantum spin Hall effect up to 100 kelvin in a monolayer crystal, Science **359**, 76 (2018).
[27] C. Xu and J. E. Moore, Stability of the quantum spin Hall effect: Effects of interactions, disorder, and Z_2 topology, Phys. Rev. B **73**, 045322 (2006).
[28] J. Maciejko, Ch. Liu, Y. Oreg, X.-L. Qi, C. Wu, and S.-C. Zhang, Kondo Effect in the Helical Edge Liquid of the Quantum Spin Hall State, Phys. Rev. Lett. **102**, 256803 (2009).
[29] Y. Tanaka, A. Furusaki, and K. A. Matveev, Conductance of a Helical Edge Liquid Coupled to a Magnetic Impurity, Phys. Rev. Lett. **106**, 236402 (2011).
[30] T. L. Schmidt, S. Rachel, F. von Oppen, and L. I. Glazman, Inelastic Electron Backscattering in a Generic Helical Edge Channel, Phys. Rev. Lett. **108**, 156402 (2012).
[31] N. Lezmy, Y. Oreg, and M. Berkooz, Single and multiparticle scattering in helical liquid with an impurity, Phys. Rev. B **85**, 235304 (2012).
[32] J. I. Väyrynen, M. Goldstein, and L. I. Glazman, Helical Edge Resistance Introduced by Charge Puddles, Phys. Rev. Lett. **110**, 216402 (2013).
[33] V. Cheianov and L. I. Glazman, Mesoscopic Fluctuations of Conductance of a Helical Edge Contaminated by Magnetic Impurities, Phys. Rev. Lett. **110**, 206803 (2013).
[34] B. L. Altshuler, I. L. Aleiner, and V. I. Yudson, Localization at the Edge of a 2D Topological Insulator by Kondo Impurities with Random Anisotropies, Phys. Rev. Lett. **111**, 086401 (2013).
[35] J. I. Väyrynen, M. Goldstein, Y. Gefen, and L. I. Glazman, Resistance of helical edges formed in a semiconductor heterostructure, Phys. Rev. B **90**, 115309 (2014).
[36] N. Kainaris, I. V. Gornyi, S. T. Carr, and A. D. Mirlin, Conductivity of a generic helical liquid, Phys. Rev. B **90**, 075118 (2014).
[37] O. M. Yevtushenko, A. Wugalter, V. I. Yudson, and B. L. Altshuler, Transport in helical Luttinger liquid with Kondo impurities, Europhys. Lett. **112**, 57003 (2015).
[38] A. Rod, T. L. Schmidt, and S. Rachel, Spin texture of generic helical edge states, Phys. Rev. B **91**, 245112 (2015).
[39] J. I. Väyrynen, F. Geissler, and L. I. Glazman, Magnetic moments in a helical edge can make weak correlations seem strong, Phys. Rev. B **93**, 241301(R) (2016).
[40] P. P. Aseev and K. E. Nagaev, Shot noise in the edge states of 2D topological insulators, Phys. Rev. B **94**, 045425 (2016).
[41] L. Kimme, B. Rosenow, and A. Brataas, Backscattering in helical edge states from a magnetic impurity and Rashba disorder, Phys. Rev. B **93**, 081301(R) (2016).
[42] J. Wang, Y. Meir, and Y. Gefen, Spontaneous Breakdown of Topological Protection in Two Dimensions, Phys. Rev. Lett. **118**, 046801 (2017).
[43] A. Mani and C. Benjamin, Probing helicity and the topological origins of helicity via non-local Hanbury-Brown and Twiss correlations, Sci. Rep. **7**, 6954 (2017).
[44] C.-H. Hsu, P. Stano, J. Klinovaja, and D. Loss, Nuclear-spin-induced localization of edge states in two- dimensional topological insulators, Phys. Rev. B **96**, 081405(R) (2017).
[45] C.-H. Hsu, P. Stano, J. Klinovaja, and D. Loss, Effects of nuclear spins on the transport properties of the edge of two-dimensional topological insulators, Phys. Rev. B **97**, 125432 (2018).
[46] P. D. Kurilovich, V. D. Kurilovich, I. S. Burmistrov, and M. Goldstein, Helical edge transport in the presence of a magnetic impurity, Pis'ma v ZhETF **106**, 575 (2017) [JETP Lett. **106**, 593 (2017)].
[47] V. D. Kurilovich, P. D. Kurilovich, I. S. Burmistrov, and M. Goldstein, Helical edge transport in the presence of a magnetic impurity: The role of local anisotropy, Phys. Rev. B **99**, 085407 (2019).
[48] O. M. Yevtushenko and V. I. Yudson, Kondo Impurities Coupled to Helical Luttinger Liquid: RKKY-Kondo Physics Revisited, Phys. Rev. Lett. **120**, 147201 (2018).
[49] S. U. Piatrusha, L. V. Ginzburg, E. S. Tikhonov, D. V. Shovkun, G. Koblmueller, A. V. Bubis, A. K. Grebenko, A. G. Nasibulin, and V. S. Khrapai, Noise insights into electronic transport, JETP Lett. **108**, 71 (2018).

[50] E. S. Tikhonov, D. V. Shovkun, V. S. Khrapai, Z. D. Kvon, N. N. Mikhailov, and S. A. Dvoretsky, Shot noise of the edge transport in the inverted band HgTe quantum wells, JETP Lett. **101**, 708 (2015).

[51] A. Del Maestro, T. Hyart, and B. Rosenow, Backscattering between helical edge states via dynamic nuclear polarization, Phys. Rev. B **87**, 165440 (2013).

[52] J. I. Väyrynen and L. I. Glazman, Current Noise from a Magnetic Moment in a Helical Edge, Phys. Rev. Lett. **118**, 106802 (2017).

[53] K. E. Nagaev, S. V. Remizov, and D. S. Shapiro, Noise in the helical edge channel anisotropically coupled to a local spin, JETP Lett. **108**, 664 (2018).

[54] R. Stühler, F. Reis, T. Müller, T. Helbig, T. Schwemmer, R. Thomale, J. Schäfer, and R. Claessen, Tomonaga-Luttinger liquid in the edge channels of a quantum spin Hall insulator, arXiv:1901.06170.

[55] D. Otten, Magnetic impurity coupled to helical edge states, Bachelor's thesis, Institute for Quantum Information, RWTH Aachen University, 2013.

[56] M. Esposito, U. Harbola, and S. Mukamel, Nonequilibrium fluctuations, fluctuation theorems, and counting statistics in quantum systems, Rev. Mod. Phys. **81**, 1665 (2009).

[57] See Supplemental Material at http://link.aps.org/supplemental/10.1103/PhysRevLett.123.056803 for a derivation of the generalized master equation governing the time evolution of the cumulant generating function of the number of backscattered electrons, analytical expressions for the backscattering current and the backscattering Fano factor, and the effect of electron-electron interaction, which includes Refs. [58–60].

[58] Á. Rivas and S. F. Huelga, *Open Quantum Systems* (Springer, New York, 2012).

[59] T. Giamarchi, *Quantum Physics in One Dimension* (Oxford University Press, Oxford, 2004).

[60] B. Probst, P. Virtanen, and P. Recher, Controlling spin polarization of a quantum dot via a helical edge state, Phys. Rev. B **92**, 045430 (2015).

[61] F. W. J. Olver, A. B. Olde Daalhuis, D. W. Lozier, B. I. Schneider, R. F. Boisvert, C. W. Clark, B. R. Miller, and B. V. Saunders, NIST Digital Library of Mathematical Functions, http://dlmf.nist.gov/, Chap. 31.